



Topological Analysis of the Type 3 Secretion System Translocon Pore Protein IpaC following Its Native Delivery to the Plasma Membrane during Infection

Brian C. Russo,^{a,b} Jeffrey K. Duncan,^a Marcia B. Goldberg^{a,b}

^aDivision of Infectious Diseases, Massachusetts General Hospital, Boston, Massachusetts, USA

^bDepartment of Microbiology, Blavatnik Institute, Harvard Medical School, Boston, Massachusetts, USA

ABSTRACT Many Gram-negative bacterial pathogens require a type 3 secretion system (T3SS) to deliver effector proteins into eukaryotic cells. Contact of the tip complex of the T3SS with a target eukaryotic cell initiates secretion of the two bacterial proteins that assemble into the translocon pore in the plasma membrane. The translocon pore functions to regulate effector protein secretion and is the conduit for effector protein translocation across the plasma membrane. To generate insights into how the translocon pore regulates effector protein secretion, we defined the topology of the *Shigella* translocon pore protein IpaC in the plasma membrane following its native delivery by the T3SS. Using single cysteine substitution mutagenesis and site-directed labeling with a membrane-impermeant chemical probe, we mapped residues accessible from the extracellular surface of the cell. Our data support a model in which the N terminus of IpaC is extracellular and the C terminus of IpaC is intracellular. These findings resolve previously conflicting data on IpaC topology that were based on nonnative delivery of IpaC to membranes. *Salmonella enterica* serovar Typhimurium also requires the T3SS for effector protein delivery into eukaryotic cells. Although the sequence of IpaC is closely related to the *Salmonella* translocon pore protein SipC, the two proteins have unique functional attributes during infection. We showed a similar overall topology for SipC and IpaC and identified subtle topological differences between their transmembrane α -helices and C-terminal regions. Together, our data suggest that topological differences among distinct translocon pore proteins may dictate organism-specific functional differences of the T3SSs during infection.

IMPORTANCE The type 3 secretion system (T3SS) is a nanomachine required for virulence of many bacterial pathogens that infect humans. The system delivers bacterial virulence proteins into the cytosol of human cells, where the virulence proteins promote bacterial infection. The T3SS forms a translocon pore in the membranes of target cells. This pore is the portal through which bacterial virulence proteins are delivered by the T3SS into the eukaryotic cytosol. The pore also regulates secretion of these virulence proteins. Our work defines the topology of translocon pore proteins in their native context during infection, resolves previously conflicting reports about the topology of the *Shigella* translocon pore protein IpaC, and provides new insights into how interactions of the pore with the T3SS likely produce signals that activate secretion of virulence proteins.

KEYWORDS IpaC, *Salmonella*, *Shigella flexneri*, SipC, topology, type 3 secretion

The type 3 secretion system (T3SS) is a specialized nanomachine required for the virulence of more than 30 bacterial pathogens (1). The T3SS translocates bacterial virulence proteins, known as effector proteins, from the bacterial cytosol into the

Citation Russo BC, Duncan JK, Goldberg MB. 2019. Topological analysis of the type 3 secretion system translocon pore protein IpaC following its native delivery to the plasma membrane during infection. mBio 10:e00877-19. <https://doi.org/10.1128/mBio.00877-19>.

Editor Vanessa Sperandio, UT Southwestern Medical Center Dallas

Copyright © 2019 Russo et al. This is an open-access article distributed under the terms of the [Creative Commons Attribution 4.0 International license](https://creativecommons.org/licenses/by/4.0/).

Address correspondence to Marcia B. Goldberg, marcia.goldberg@mgh.harvard.edu. This article is a direct contribution from a Fellow of the American Academy of Microbiology. Solicited external reviewers: Peggy Cotter, University of North Carolina at Chapel Hill; Arne Rietsch, Case Western Reserve University.

Received 9 April 2019

Accepted 22 April 2019

Published 28 May 2019

cytosol of eukaryotic cells. The T3SS is composed of a base that spans the two bacterial membranes (2), a needle that is anchored in the base and extends away from the bacterial surface (2, 3), and a tip complex that prevents nonspecific secretion (4, 5). Upon contact of the tip complex with a eukaryotic cell, the T3SS secretes two bacterial proteins that embed in the plasma membrane (6), where they assemble into a heterooligomeric pore, known as the translocon pore (3). The translocon pore is essential for T3SS activity; it functions as a conduit through which bacterial virulence proteins ("effectors") traverse the plasma membrane to gain access to the eukaryotic cytosol (3), and it participates in defining the timing of the secretion of these effectors by the T3SS (7).

Shigella flexneri causes bacterial dysentery in humans and requires a T3SS to invade into and spread among the epithelial cells of the colon. *S. flexneri* has become a model organism with which to investigate T3SS structure and function. The *S. flexneri* translocon pore is composed of the proteins IpaB and IpaC. Interactions of IpaC with host intermediate filaments are required for the *Shigella* T3SS to stably associate with the translocon pore in a process known as docking (7). Docking is essential for the bacterium to remain adherent to the cell and to secrete virulence proteins through the T3SS (7, 8). Thus, stable interactions of the T3SS needle with the pore cue the T3SS to activate secretion. Aspects of the pore accessible from the extracellular environment are predicted to interact with the needle, but it is uncertain how this interaction occurs, as the topology of IpaC in the plasma membrane is controversial. The two previous studies that investigated IpaC topology used purified recombinant IpaC. These studies showed IpaC inserting into the membrane with its N terminus on the extracellular surface of the plasma membrane, but they came to opposing conclusions about the location of the C terminus; the study of interactions of IpaC with artificial liposomes concluded that IpaC contained a single transmembrane α -helix with the C terminus present in the liposome lumen (9), whereas investigation of purified IpaC incorporating into macrophage membranes concluded that IpaC contained two transmembrane α -helices with the C terminus accessible on the extracellular surface of the macrophage (10).

Here we defined the topology of the *Shigella* translocon protein IpaC during bacterial infection following its native delivery into the plasma membrane by the T3SS. Using single cysteine accessibility mutagenesis, we defined a topological map of IpaC showing that the amino-terminal region is extracellular, that the carboxy-terminal region is in the cytosol, and that a single transmembrane α -helix is present. Furthermore, to test whether this topology is conserved among IpaC homologs in other pathogens that require T3SS for virulence, the accessibility of analogous residues for the *Salmonella* pore protein SipC was tested. We found that the overall topologies of IpaC and SipC are similar. However, we observed subtle differences between the two proteins in the accessibility of the transmembrane α -helices and the C-terminal regions that may contribute to organism-specific functional differences of these T3SSs during infection.

RESULTS

Generation of single cysteine substitution derivatives of IpaC. To generate insights into how the translocon pore regulates effector protein secretion, the accessibility of specific residues within natively delivered plasma membrane-embedded IpaC was determined. IpaC residues were selected for analysis based on a combination of previous *in silico* analysis of the putative IpaC secondary structure (7) (Fig. 1A), and since our approach involved single cysteine substitution, on previous successful mutation of particular IpaC residues (9, 11) and an attempt to minimize the negative impact of the cysteine substitution on protein function by choosing alanine or serine residues for replacement.

IpaC tolerates substitution with cysteine at numerous sites along the length of the protein. Selected IpaC residues were replaced with cysteine, and the accessibility of these cysteines was determined by site-directed labeling with a chemical probe

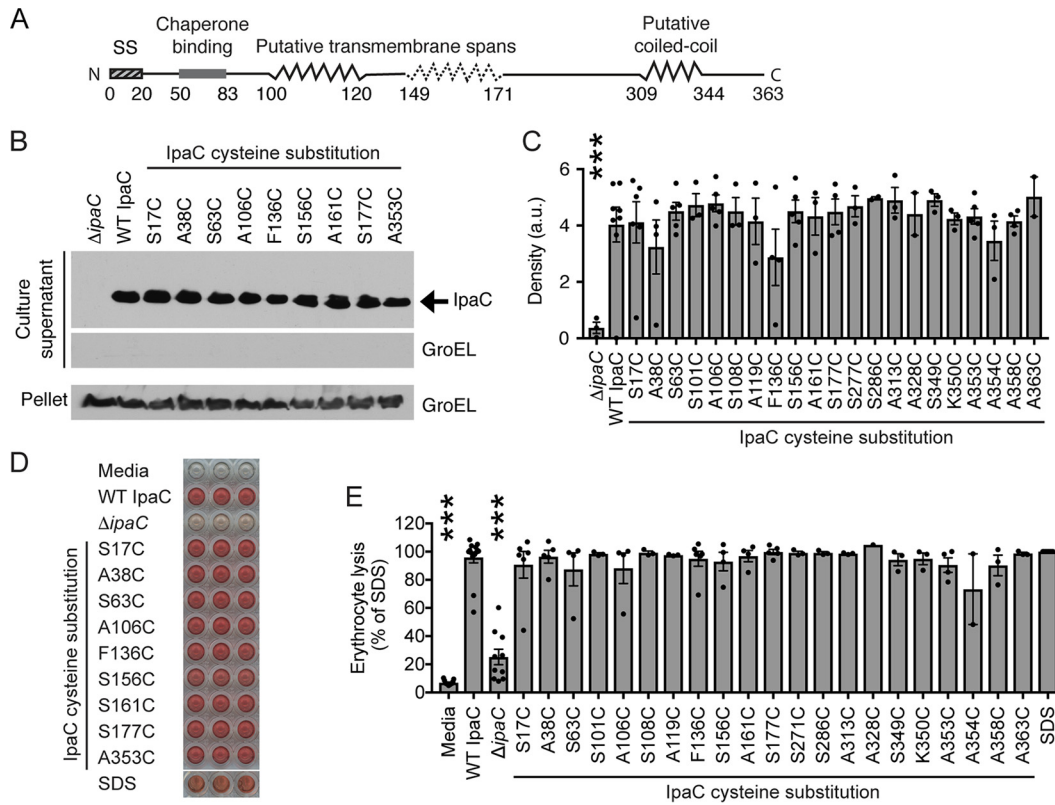


FIG 1 Cysteine substitution derivatives of IpaC support secretion and formation of translocon pores with efficiencies similar to those of wild-type (WT) IpaC. (A) Schematic showing the putative secondary structure of IpaC (7, 9). Putative transmembrane span, residues 100 to 120 (solid zigzag), predicted by *in silico* analyses and experimental data (7, 9); second putative transmembrane span, residues 149 to 171 (dotted zigzag), suggested by Kuwae et al. (10). (B and C) The efficiency by which each IpaC cysteine substitution derivative or WT IpaC, expressed in the *S. flexneri* ΔIpaC mutant strain, was secreted through the T3SS following activation of secretion by the addition of Congo red to the medium. Soluble IpaC was found in the culture supernatant. (B) Representative Western blots. IpaC and GroEL, bacterial cytosolic protein used as a control for bacterial lysis (culture supernatant) and for loading (pellet). (C) Densitometry analysis of bands for soluble secreted IpaC from three independent experiments for each cysteine substitution derivative. Density is shown in arbitrary units (a.u.). Values are means ± standard error of the means (SEM) (error bars). Black dots represent the values for individual experimental replicates. ***, $P < 0.001$ (by ANOVA with Dunnett's *post hoc* test comparing detected IpaC secreted from *S. flexneri* ΔIpaC strain to *S. flexneri* ΔIpaC strain producing WT IpaC). Secretion of IpaC cysteine substitution derivatives was not significantly different from WT IpaC (by ANOVA with Dunnett's *post hoc* test). (D and E) Erythrocytes were cocultured with *S. flexneri* ΔIpaC strains producing IpaC containing a cysteine substitution derivative or WT IpaC; pore formation causes erythrocyte lysis and hemoglobin release. (D) Representative image showing hemoglobin released from erythrocytes. Each independent experiment was performed in triplicate. (E) The abundance of hemoglobin released was quantified by A_{570} from at least two independent experiments for each cysteine substitution mutant. Values are means ± SEM. Black dots represent the values for independent experimental replicates. ***, $P < 0.001$ comparing hemoglobin release induced by the indicated strains to hemoglobin release induced by the *S. flexneri* strain producing WT IpaC (by ANOVA with Dunnett's *post hoc* test). Hemoglobin release induced by each strain producing cysteine substitution derivatives of IpaC was not statistically different from hemoglobin release induced by the strain producing WT IpaC (by ANOVA with Dunnett's *post hoc* test).

specific for the thiol group of the cysteine (12). Of note, native IpaC lacks cysteines. During infection, together with IpaB, IpaC is secreted through the T3SS and embeds in and forms a pore in the plasma membrane. Type 3 substrates are secreted through the T3SS needle in an unfolded conformation, and proteins that are folded cannot traverse the needle (13). When the T3SS was artificially activated by incubation of bacteria with the dye Congo red (14), all IpaC cysteine substitution derivatives were readily secreted through the type 3 secretion needle into the culture supernatant (Fig. 1B and C), indicating that the cysteine substitutions did not disrupt or only minimally disrupted protein conformation in the bacterium.

The ability of the cysteine substitution derivatives of IpaC to support formation of translocon pores in plasma membranes was tested using the membranes of erythrocytes by coculturing erythrocytes with strains of *S. flexneri* producing individual IpaC

cysteine substitution derivatives. In this assay, the formation of translocon pores in the membranes of the erythrocytes leads to lysis of the erythrocyte and release of hemoglobin. The abundance of hemoglobin released into the infection media, quantified spectrophotometrically, is an indicator of the efficiency of cell lysis. The absorbance of the supernatants was similar for strains of *S. flexneri* producing IpaC cysteine substitution derivatives and wild-type (WT) IpaC (Fig. 1D and E), which indicates that the IpaC derivatives support formation of translocon pores at efficiencies similar to that of WT IpaC.

To test the impact of the cysteine substitutions on the function of the translocon pores, translocon pore-related functions during infection of cells by *S. flexneri* were assessed. In a process termed docking (7, 8, 15), *Shigella* stably associates with eukaryotic cells via interactions between the T3SS needle and the translocon pore; IpaC is required for docking and subsequent effector translocation (Fig. 2A to D) (7). To test whether IpaC cysteine substitution derivatives supported docking, HeLa cells were infected with strains of *S. flexneri* producing an IpaC substitution derivative or WT IpaC, and the number of bacteria that stably associated with cells at 40 min of infection was quantified. *S. flexneri* strains producing an IpaC with a substituted cysteine docked to cells at numbers similar to those of *S. flexneri* producing WT IpaC (Fig. 2A and E).

The ability of T3SS translocon pores formed by the IpaC cysteine substitution derivatives to activate effector secretion was monitored using a fluorescent transcription-based reporter of T3SS activity (TSAR) (7, 16); following the secretion of the translocon pore proteins and the bacterial effector protein OspD through the T3SS, the TSAR reporter produces green fluorescent protein (GFP) in the bacterium. The promoter for GFP is regulated by MxiE, which is activated upon secretion of OspD (16). *S. flexneri* producing cysteine substituted IpaC derivatives activated the T3SS to secrete effector proteins at efficiencies similar to those of WT IpaC (Fig. 2A, F, and G; see also Fig. S1A in the supplemental material). Both the absolute number per cell of bacteria with active secretion (Fig. 2A and F) and the percentage of docked bacteria with active secretion (Fig. 2A and G) were similar for *S. flexneri* producing IpaC containing cysteine substitutions and *S. flexneri* producing WT IpaCs. These data demonstrate that cysteine substitution at the selected residues in IpaC did not adversely affect T3SS-mediated docking or secretion of effector proteins through the T3SS, including through the translocon pore.

Shigella invasion of cells requires the translocation of bacterial effector proteins through the translocon pore into the cytosol. The translocated effectors induce actin rearrangements, which in turn generate membrane ruffles that engulf the bacteria (17–19). The effect of cysteine substitutions in IpaC on *S. flexneri* invasion was tested by quantifying the numbers of bacteria internalized during infection of HeLa cells (7). The numbers of intracellular bacteria recovered were similar for HeLa cells infected with *S. flexneri* producing IpaC cysteine substitution derivatives and those infected with *S. flexneri* producing WT IpaC (Fig. S1B). In sum, substitution of selected IpaC residues with cysteine did not significantly alter either IpaC activity or T3SS function during *S. flexneri* infection of cells.

Accessibility of IpaC residues in membrane-embedded *S. flexneri* translocon pores. To measure the accessibility of IpaC residues in translocon pores embedded in the plasma membranes of host cells, site-directed labeling by methoxypolyethelene glycol maleimide (PEG5000-maleimide) was performed with the library of IpaC cysteine substitution derivatives characterized above. Because PEG5000-maleimide is membrane impermeant (12) and is too big to pass entirely through the translocon pore (3, 7), this approach specifically assesses the accessibility of the cysteine residue to the extracellular surface of the eukaryotic cell. Cysteine substitutions within the N-terminal domain (residues 1 to 99) of IpaC labeled efficiently with PEG5000-maleimide, as demonstrated by a distinct shift to a slower migrating position by SDS-PAGE (Fig. 3). Efficient labeling was also observed for one of the four residues tested within the putative transmembrane α -helix (residues 100 to 120) (Fig. 3); labeling at IpaC A106C was efficient, whereas labeling of the three other residues in the putative transmem-

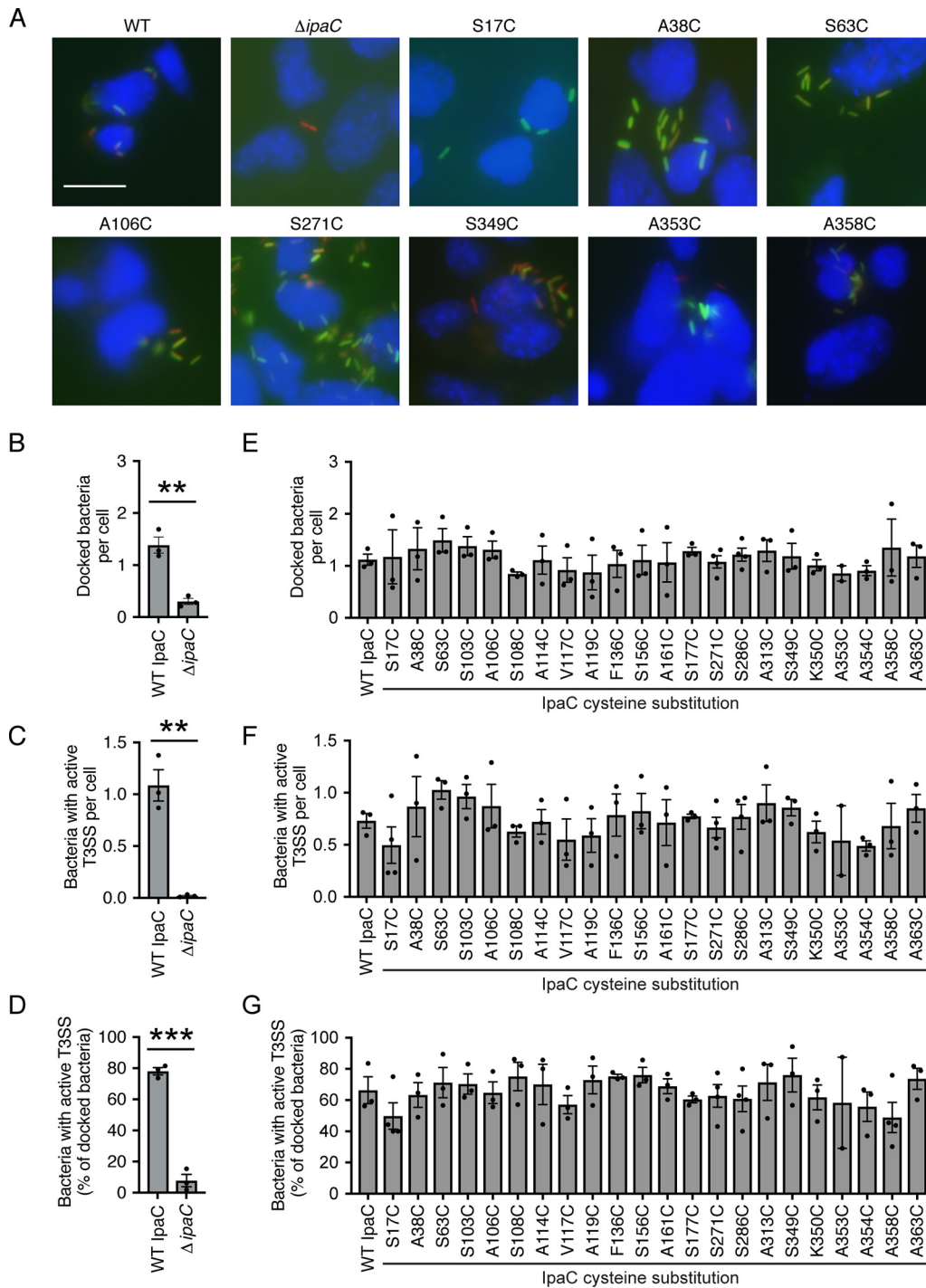


FIG 2 Cysteine substitution derivatives of IpaC support formation of translocon pores that function similar to those formed by WT IpaC. Stable docking and effector translocation upon infection of mouse embryonic fibroblast cells with *S. flexneri* $\Delta ipaC$ strains producing IpaC derivatives containing a cysteine substitution derivative or WT IpaC. The secretion activity of the T3SS was measured using the TSAR reporter (7, 16). (A) Representative images of infected cells. DNA (blue), mCherry (all bacteria) (red), and GFP (TSAR reporter; bacteria with active T3SS secretion) (green) are shown. Bar, 20 μ M. (B and E) Average number of bacteria that stably associated with cells (docked). The number of red fluorescent protein (RFP)-positive bacteria per cell is shown. (C and F) Average number per cell of bacteria that produced GFP, indicating active T3SS secretion. The number of GFP-positive bacteria per cell is shown. (D and G) The percentage of docked bacteria that produced GFP, indicating active T3SS secretion. The number of GFP-positive bacteria per RFP-positive bacterium is shown. Values are means \pm SEM. Black dots represent the values for independent experimental replicates. Values that are significantly different by Student's *t* test are indicated by asterisks as follows: **, $P < 0.01$; ***, $P < 0.001$. Stable docking of bacteria and secretion via the T3SS for each strain producing an IpaC cysteine substitution derivative was not statistically different from that of the strain producing WT IpaC (by ANOVA).

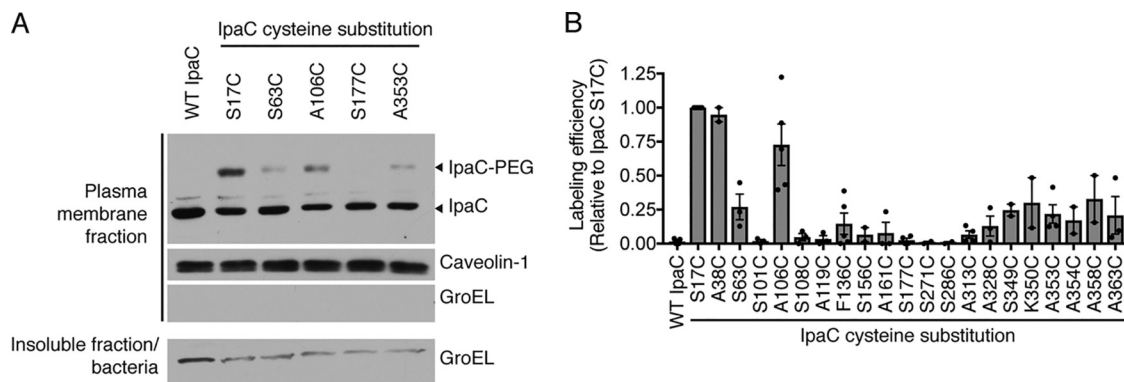


FIG 3 Topology of membrane-embedded IpaC upon native delivery of the translocon pore. Accessibility of membrane-embedded IpaC to labeling with PEG5000-maleimide upon infection of HeLa cells with *S. flexneri*. *S. flexneri* Δ IpaC strains producing IpaC cysteine substitution mutants or WT IpaC are shown. (A) Gel shift of PEG5000-maleimide-labeled IpaC in the plasma membrane fraction of infected HeLa cells. Representative Western blots are shown. The positions of IpaC labeled with PEG5000-maleimide (IpaC-PEG), unlabeled IpaC (IpaC), caveolin-1, a eukaryotic plasma membrane protein, and GroEL, a bacterial cytosolic protein, are shown to the right of the gel. (B) Relative accessibility of IpaC cysteine substitutions. Densitometry analysis of IpaC-PEG5000 bands from two to five independent experiments for each cysteine substitution derivative. Values are means \pm SEM. Black dots represent the values for independent experimental replicates.

brane α -helix that were tested (S101C, S108C, and A119C) was essentially not detected. The labeling of IpaC cysteine substitutions C terminal to the putative transmembrane α -helix was weak, except among substitutions of the 15 residues closest to the C terminus (residues 349 to 363) (Fig. 3). All cysteine substitutions of IpaC, including the substitutions in the putative transmembrane α -helix and the substitutions C terminal to it, were readily labeled by PEG5000-maleimide when the labeling was performed on IpaC in solution following secretion from bacteria *in vitro* (Fig. S2A and B), indicating that the lack of labeling observed during infection was a function of inaccessibility due to the membrane-embedded state rather than to fundamental inaccessibility of the residue in the protein *per se*. When labeling was performed following permeabilization of the plasma membrane, accessibility of IpaC residues near the C terminus was similar to the accessibility of the residues in the N-terminal domain (Fig. S2C and D), which demonstrates that under nonpermeabilizing conditions, the plasma membrane inhibited access of PEG5000-maleimide to the residues near the C terminus. To test whether docking of the needle on the translocon pore inhibited labeling of residues near the C terminus, we compared the accessibility of IpaC A358C, which is close to the C terminus (R362), with that of S17C, a residue in the N-terminal domain, in the presence and absence of intermediate filaments. We previously showed that in the absence of intermediate filaments, docking does not occur but translocon pores form at wild-type levels (7). Since docking occurs through interactions of the needle tip complex with the pore (15), in the absence of intermediate filaments, pores form without a needle tip complex associated with the pore. The accessibility of A358C was similar in the presence and absence of intermediate filaments (Fig. S3), and the accessibility of S17C was greater than the accessibility of A358C and was also independent of intermediate filaments (Fig. S3). These data show that the engagement of the T3SS needle and/or tip complex with the translocon pore does not alter the accessibility of residues near the C terminus of IpaC. Altogether, these results indicate that, whereas IpaC sequences immediately C terminal to the putative transmembrane α -helix are intracellular, some or all of the 15 residues closest to the C terminus of IpaC are partially accessible from the extracellular surface of the plasma membrane.

Accessibility of *Salmonella* translocon pore protein SipC in membrane-embedded *Salmonella* translocon pores. The *Shigella* T3SS is closely related to the *Salmonella* T3SS (1). The translocon pore of *Salmonella* is composed of SipB and SipC, with SipB being homologous to IpaB and SipC being homologous to IpaC. Alignment of SipC and IpaC by Clustal Omega (20–22) showed that 33% of IpaC residues are

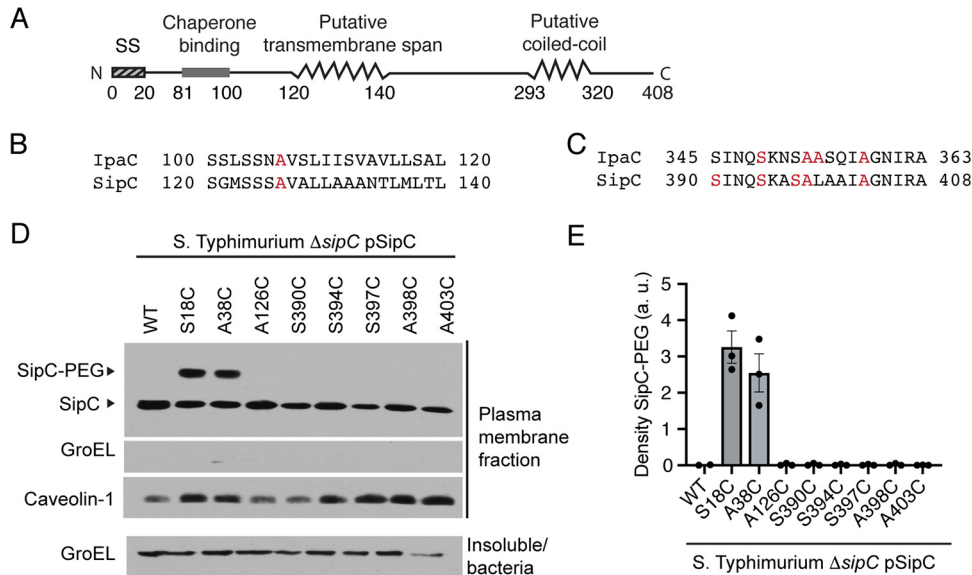


FIG 4 SipC is inserted in the plasma membrane with the N-terminal domain extracellular and the C-terminal domain intracellular. (A) Schematic showing the putative secondary structure of SipC. (B and C) Alignment by Clustal Omega of IpaC and SipC showing the putative transmembrane α -helix (B) and C-terminal 19 amino acids (C). Red lettering indicates sites of individual cysteine substitutions analyzed in this paper. (D and E) Accessibility of membrane-embedded SipC residues to the extracellular surface of the plasma membrane. Labeling of SipC with PEG5000-maleimide upon infection of HeLa cells with *S. Typhimurium* $\Delta sipC$ producing SipC cysteine substitution derivatives or WT SipC is shown. (D) Gel shift of PEG5000-maleimide-labeled SipC in the plasma membrane fraction of infected HeLa cells. Representative Western blots are shown. The positions of SipC labeled with PEG5000-maleimide (SipC-PEG), unlabeled SipC (SipC), caveolin-1, a eukaryotic plasma membrane protein, and GroEL, a bacterial cytosolic protein, are shown to the left of the gel. (E) Relative accessibility of SipC cysteine substitutions. Densitometry analysis of SipC-PEG5000 bands from three independent experiments for each cysteine substitution derivative. Values are means \pm SEM. Black dots represent the values for independent experimental replicates.

identical to those in SipC and another 26% of IpaC residues retain functional properties similar to those in SipC, together yielding 52% amino acid similarity of IpaC to SipC (Fig. S4). Both proteins are required for translocon pore formation, docking, and effector protein secretion; however, transcomplementation experiments show that the two proteins do not function equivalently in all aspects of infection. Whereas *Salmonella enterica* serovar Typhimurium is predominantly found within vacuoles, complementation of an *S. Typhimurium sipC* mutant with *Shigella ipaC* enables bacterial escape from the vacuole (23), which indicates that SipC and IpaC are sufficient to direct the bacterium to distinct intracellular niches (23).

To explore whether the observed functional differences between IpaC and SipC were associated with differences in protein topology in the plasma membrane, we compared the accessibility of SipC residues with that of IpaC residues. Like IpaC, native SipC lacks cysteines. The putative secondary structure of SipC is very similar to that of IpaC, with a putative N-terminal extracellular domain (residues 1 to 119), a putative transmembrane α -helix (residues 120 to 140), and C terminal to the transmembrane α -helix, a putative coiled-coil domain (residues 293 to 320) (Fig. 4A). The second putative transmembrane span identified in IpaC was not clearly delineated by *in silico* analyses of SipC. We substituted cysteines at residues of SipC that were analogous to those chosen for substitution in IpaC (Fig. 4B and C). During *S. Typhimurium* infection of HeLa cells, the accessibility of these residues from the extracellular surface of the plasma membrane was tested using the same method used for IpaC, site-directed labeling with PEG5000-maleimide. As observed for IpaC, substitutions in the N-terminal domain of SipC labeled efficiently (Fig. 4D and E). In contrast to our findings for IpaC, labeling was not observed for any other SipC substitution tested (Fig. 4D and E); this included SipC A126C, a cysteine substitution at a residue within the SipC putative transmembrane α -helix that is analogous to IpaC A106C, which labeled efficiently with

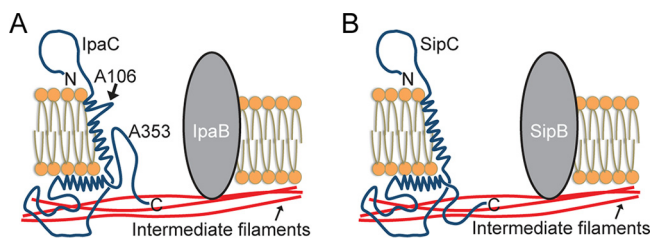


FIG 5 Topological models of plasma membrane-embedded *Shigella* IpaC and plasma membrane-embedded *Salmonella* SipC. (A) Topological model of the *Shigella* translocon pore protein IpaC. The N-terminal domain of IpaC is situated on the extracellular side of the membrane, which is shown at the top of the figure. A single transmembrane α -helix is present. IpaC A106 is positioned such that it is accessible to the lumen of the pore. The region C terminal to the transmembrane α -helix, including the coiled-coil domain, is situated on the cytosolic side of the membrane, which is shown at the bottom of the figure. IpaC A353, which is among the C-terminal 15 residues, is present within a loop of IpaC that is positioned within the pore lumen and accessible to the extracellular side of the plasma membrane. (B) Topological model of the *Salmonella* translocon pore protein SipC. The N-terminal domain of SipC is situated on the extracellular side of the plasma membrane. A single transmembrane α -helix is present. The C-terminal domain is situated on the cytosolic side of the plasma membrane.

PEG5000-maleimide, and cysteine substitutions at residues within the C-terminal 15 amino acids of SipC, which in IpaC labeled with intermediate efficiency.

As for IpaC, SipC tolerated substitution with cysteine at numerous sites along the length of the protein. The SipC cysteine derivatives were produced in *Salmonella* at levels similar to WT SipC (Fig. S5A). Moreover, each cysteine substitution derivative supported *S. Typhimurium* docking to HeLa cells (Fig. S5B). Thus, the differences in labeling observed for cysteine substitutions of IpaC compared to cysteine substitutions of SipC were not due to altered function of the SipC derivatives.

These data suggest that the overall topologies of plasma membrane-embedded SipC and plasma membrane-embedded IpaC are similar. For each protein, the N-terminal domain is extracellular, a single transmembrane α -helix is present, and the C terminus is intracellular (Fig. 5). Despite the similarities in overall topology, the differences observed in the accessibility of substitutions close to the C termini of the two proteins suggest that subtle topological or structural differences exist in the transmembrane α -helix and C-terminal regions. The differences we observe between the two proteins in the context of plasma membrane-embedded translocon pores may be relevant to functional differences observed for *Shigella* and *Salmonella* translocon pores.

DISCUSSION

The T3SS is essential for the pathogenesis of many important human bacterial pathogens, and the translocon pore is essential for T3SS function. To generate insights into how the translocon pore participates in the signaling that activates secretion of effector proteins, we defined the topology of IpaC in the membranes of human-derived cells. To our knowledge, this represents the first detailed topological analysis of a type 3 translocon pore protein following its native delivery to the plasma membrane. We show that the N-terminal region of IpaC is extracellular and the C-terminal region of IpaC is in the host cytosol. Moreover, we observed a similar overall topology for SipC, the IpaC homolog in *Salmonella*. The observation that the N-terminal region of IpaC is located on the extracellular side of the plasma membrane is consistent with previous observations investigating the interactions of recombinant IpaC with the membrane (9, 10).

The labeling of A106C in the transmembrane span indicates that the outer portion of the pore channel is at least 4.4 nm wide, the approximate size of PEG5000-maleimide. Moreover, the lack of labeling for other residues in the transmembrane α -helix of IpaC suggests that toward the cytosolic side of the plasma membrane, either the lumen of the pore becomes narrower, such that the PEG5000-maleimide is precluded from accessing the IpaC residues, and/or that other IpaC residues do not line the

pore interior. If the latter were true, it could indicate that IpaB residues line the bulk of the channel.

C terminal to the predicted transmembrane α -helix are sequences without predicted secondary structure (residues 121 to 308) and a predicted coiled-coil domain (residues 309 to 344). The minimal accessibility to PEG5000-maleimide of IpaC cysteine substitutions within these sequences strongly suggests that these sequences, including the coiled-coil domain, lie within the cytosol and that residues 100 to 120 constitute a transmembrane α -helix and the only transmembrane α -helix in the protein. By extension, these data suggest that all of IpaC C terminal to this transmembrane α -helix lies on the cytosolic side of the plasma membrane (Fig. 5A). Additional attempts to directly assess the location of the C-terminal region of IpaC, including limited proteolysis, incorporation of enzymatic cleavage sites that would specifically function within the intracellular environment, and immunolabeling with monoclonal antibodies specific for C-terminal or N-terminal sequences, were uninformative.

Cysteine substitutions in the C-terminal 15 amino acids of IpaC were weakly but reproducibly accessible from outside the cell, suggesting that they are present within the pore lumen. Consistent with this possibility, cross-linking studies showed that residues in the C-terminal region of the *Pseudomonas* translocon pore protein PopD, a homolog of IpaC, interact with the *Pseudomonas* T3SS tip complex protein (15), which docks onto the extracellular face of the translocon pore. Of note, atomic force microscopy studies suggest that the lumen of the *Escherichia coli* translocon pore is shaped like a funnel, with the narrower portion of the funnel closer to the cytosolic side of the plasma membrane (24). If the *Shigella* translocon pore is shaped similarly to the *E. coli* translocon pore, the detection of PEG5000-maleimide labeling of cysteine substitutions near the C terminus of IpaC could be consistent with these residues looping back from the cytosolic side of the plasma membrane into the pore lumen where they might be positioned to engage the tip complex. If this is the case, these C-terminal domain residues might contribute directly to the narrowest portion of the funnel shape of the pore.

Our data support a model of the native topology of IpaC in mammalian plasma membranes in which the N-terminal domain of IpaC is extracellular, a single transmembrane α -helix crosses the plasma membrane, the region C terminal to the transmembrane α -helix is present within the cytosol, and the C-terminal 15 amino acids of IpaC reenter the pore interior (Fig. 5A).

The overall topologies of SipC and IpaC were similar, with the N terminus of SipC extracellular and the C terminus intracellular (Fig. 5B). Both IpaC and SipC support bacterial docking to cells (7, 8). Our models place the N-terminal regions of these proteins at the cell surface where these sequences would be positioned adjacent to the T3SS needle as it docks on the extracellular face of the translocon pore. This proximity would facilitate the involvement of the N-terminal domains of these proteins in docking and activation of effector secretion. Moreover, for both *Shigella* IpaC and *Salmonella* SipC, an interaction with intermediate filaments is required for bacterial docking (7). For IpaC, we previously demonstrated that sequences adjacent to the protein's C terminus are required for this interaction with intermediate filaments (7). Our models for IpaC and SipC place the extreme C-terminal regions of these proteins in the cytosol of the eukaryotic cell, adjacent to the intermediate filaments of the cell cortex with which they interact.

The similarity between the overall topology of IpaC and that of SipC suggests that the mechanism(s) required to deliver the two proteins into the membrane, multimerize into the pore, interact with the lipid membrane, support effector translocation, and generate signals to activate secretion may be similar. However, in contrast to the accessibility of some cysteine substitutions in the C-terminal region of IpaC, substitutions near the C terminus of SipC were completely inaccessible. This indicated that multiple topologies of SipC do not occur at an efficiency that was detected in this assay and, by extension, that the weak labeling observed at IpaC substitutions near the C terminus are unlikely to be the result of a minority population of membrane-embedded

IpaC having an alternate topology. In addition, whereas the two proteins are homologs, they display functional differences. When IpaC and SipC are swapped, IpaC partially complements the loss of SipC, but SipC is unable to complement the loss of IpaC (23, 25), and IpaC production in *S. Typhimurium* heterologously enables the bacterium to lyse the vacuolar membrane (23). Together, our findings raise the possibility that the observed subtle differences in the topological arrangements of SipC and IpaC may contribute to their functional differences during bacterial infection. We speculate that the greater accessibility in IpaC of residues within the transmembrane α -helix and near the C terminus reflects a more open channel in *Shigella* translocon pores than in *Salmonella* translocon pores. Such a conformation may be associated with lysis of the vacuolar membrane in the case of *Shigella* and maintenance of the vacuolar membrane in the case of *Salmonella*. Further investigations into translocon pore structure will inform the molecular mechanisms that drive the functional differences among the translocon pore proteins.

MATERIALS AND METHODS

Bacterial culture. Bacterial strains used in this study are described in Table 1. The wild-type *Shigella flexneri* strain was serotype 2a strain 2457T (26), and all mutants were isogenic derivatives of it. *S. flexneri* strains were cultured in Trypticase soy broth (Becton Dickinson) at 37°C. *ipaC* derivatives were encoded by genes on the pBAD33 plasmid, and their expression was driven from the pBAD promoter, induced with 1.2% arabinose. The sequences of primers used for PCR and sequencing are available from the authors upon request. The wild-type *Salmonella enterica* serovar Typhimurium strain was SL1344, and all *S. Typhimurium* mutants used in this study were isogenic derivatives of it. *Salmonella* strains were cultured in Trypticase soy broth at 37°C. *sipC* derivatives were encoded by genes on the pBAD18 plasmid, and their expression was driven from the pBAD promoter, induced with 1.2% arabinose.

Cell culture. Mouse embryonic fibroblasts were kindly provided by Victor Faundez (Emory), and HeLa (CCL2) cells were obtained from ATCC. All cells were cultured in Dulbecco's modified Eagle's medium (DMEM) supplemented with 0.45% glucose and 10% heat-inactivated fetal bovine serum (FBS); they were maintained at 37°C in humidified air containing 5% CO₂. All cells in the laboratory are periodically tested for mycoplasma; cells that test positive are treated or discarded.

Secretion assays. To assess the ability of the type 3 secretion system to secrete proteins in the absence of eukaryotic cells, the T3SS was artificially activated by the addition of Congo red (7, 14, 27). Overnight cultures were back diluted, induced where appropriate with 1.2% arabinose, and cultured for 2 h at 37°C. Bacterial cultures were normalized by optical density at 600 nm (OD₆₀₀), resuspended in phosphate-buffered saline (PBS) containing 1.2% arabinose, where appropriate, and 10 μ M Congo red, and incubated in a water bath at 37°C for 45 min. The bacteria were removed by centrifugation, and the resulting supernatant containing the secreted proteins was collected.

Erythrocyte lysis assay. Pore formation in sheep erythrocyte membranes was monitored by assessing the efficiency of erythrocyte lysis (3, 7). Briefly, 10⁸ erythrocytes were washed with saline and infected with *S. flexneri* at a multiplicity of infection (MOI) of 25 in 30 mM Tris (pH 7.5). The bacteria were centrifuged onto the erythrocytes at 2,000 $\times g$ for 10 min at 25°C. Bacteria and erythrocytes were cultured together for 30 min at 37°C in humidified air with 5% CO₂. The bacterial and erythrocyte cocultures were mixed by pipetting and then centrifuged again at 2,000 $\times g$ for 10 min at 25°C. As a positive control for lysis, an aliquot of uninfected erythrocytes was treated with 0.02% SDS and then centrifuged. The supernatants were collected, and the abundance of hemoglobin released was measured spectrophotometrically at A₅₇₀ using a Wallac 1,420 Victor² microplate reader (Perkin Elmer).

Translocation and docking. Mouse embryonic fibroblasts (MEFs) were seeded at 3 $\times 10^5$ cells per well on coverslips in a six-well plate. The cells were infected with exponential-phase *S. flexneri* (18, 28) harboring the TSAR reporter (16) at an MOI of 200. The TSAR reporter, which expresses green fluorescent protein (GFP) when the bacterial effector OspD is secreted through the T3SS (16), is an indicator of active T3SS secretion. Bacteria were centrifuged onto cells at 800 $\times g$ for 10 min at 25°C. The bacteria and cells were cocultured for an additional 30 min at 37°C in humidified air with 5% CO₂. Cells were washed three times with PBS, fixed with 3.7% paraformaldehyde for 20 min at 25°C, and washed again with PBS. DNA was stained with Hoechst. Four random microscopic fields per experimental condition were imaged by fluorescence microscopy using a Nikon Eclipse TE-300 with appropriate filters. All bacteria produced mCherry, and bacteria in which T3SS secretion was activated produced GFP (16). For each condition of each independent experiment, 20 to 250 eukaryotic cells and 20 to 210 bacteria were analyzed.

Quantification of intracellular bacteria. HeLa cells were seeded at 1.5 $\times 10^4$ cells per well in 96-well plates the day prior to infection. *S. flexneri* strains were grown as described above and added to cell monolayers in Hanks balanced salt solution (HBSS) supplemented with 1.2% arabinose at an MOI of 100. Bacteria were centrifuged onto cells for 10 min at 2,000 rpm and incubated at 37°C with 5% CO₂ for 20 min. Bacteria that did not invade the cells were removed by washing with HBSS. The HeLa cells and bacteria were cocultured for an additional hour at 37°C with fresh HBSS containing 25 μ g/ml gentamicin, which kills extracellular but not intracellular bacteria. Infected monolayers were then washed with phosphate-buffered saline and lysed in PBS containing 0.5% Triton X-100 to release the intracellular

TABLE 1 Bacterial strains used in this study

Bacterial strain	Plasmid 1	Plasmid 2	Source	Reference
<i>S. flexneri</i> 2457T	pBR322-Afa-1		Laboratory stock	7
<i>S. flexneri</i> 2457T Δ ipaC	pBR322-Afa-1		This study	This study
<i>S. flexneri</i> 2457T Δ ipaC	pBR322-Afa-1	pBAD33-IpaC	This study	This study
<i>S. flexneri</i> 2457T Δ ipaC	pBR322-Afa-1	pBAD33-IpaC S17C	This study	This study
<i>S. flexneri</i> 2457T Δ ipaC	pBR322-Afa-1	pBAD33-IpaC A38C	This study	This study
<i>S. flexneri</i> 2457T Δ ipaC	pBR322-Afa-1	pBAD33-IpaC S63C	This study	This study
<i>S. flexneri</i> 2457T Δ ipaC	pBR322-Afa-1	pBAD33-IpaC S101C	This study	This study
<i>S. flexneri</i> 2457T Δ ipaC	pBR322-Afa-1	pBAD33-IpaC S103C	This study	This study
<i>S. flexneri</i> 2457T Δ ipaC	pBR322-Afa-1	pBAD33-IpaC A106C	This study	This study
<i>S. flexneri</i> 2457T Δ ipaC	pBR322-Afa-1	pBAD33-IpaC S108C	This study	This study
<i>S. flexneri</i> 2457T Δ ipaC	pBR322-Afa-1	pBAD33-IpaC A119C	This study	This study
<i>S. flexneri</i> 2457T Δ ipaC	pBR322-Afa-1	pBAD33-IpaC F136C	This study	This study
<i>S. flexneri</i> 2457T Δ ipaC	pBR322-Afa-1	pBAD33-IpaC S156C	This study	This study
<i>S. flexneri</i> 2457T Δ ipaC	pBR322-Afa-1	pBAD33-IpaC A161C	This study	This study
<i>S. flexneri</i> 2457T Δ ipaC	pBR322-Afa-1	pBAD33-IpaC S177C	This study	This study
<i>S. flexneri</i> 2457T Δ ipaC	pBR322-Afa-1	pBAD33-IpaC S271C	This study	This study
<i>S. flexneri</i> 2457T Δ ipaC	pBR322-Afa-1	pBAD33-IpaC S286C	This study	This study
<i>S. flexneri</i> 2457T Δ ipaC	pBR322-Afa-1	pBAD33-IpaC A313C	This study	This study
<i>S. flexneri</i> 2457T Δ ipaC	pBR322-Afa-1	pBAD33-IpaC A328C	This study	This study
<i>S. flexneri</i> 2457T Δ ipaC	pBR322-Afa-1	pBAD33-IpaC S349C	This study	This study
<i>S. flexneri</i> 2457T Δ ipaC	pBR322-Afa-1	pBAD33-IpaC K350C	This study	This study
<i>S. flexneri</i> 2457T Δ ipaC	pBR322-Afa-1	pBAD33-IpaC A353C	This study	This study
<i>S. flexneri</i> 2457T Δ ipaC	pBR322-Afa-1	pBAD33-IpaC A354C	This study	This study
<i>S. flexneri</i> 2457T Δ ipaC	pBR322-Afa-1	pBAD33-IpaC A358C	This study	This study
<i>S. flexneri</i> 2457T Δ ipaC	pBR322-Afa-1	pBAD33-IpaC A363C	This study	This study
<i>S. flexneri</i> 2457T Δ ipaC	pTSAR	pBAD33	Laboratory stock	7
<i>S. flexneri</i> 2457T Δ ipaC	pTSAR	pBAD33-IpaC	Laboratory stock	7
<i>S. flexneri</i> 2457T Δ ipaC	pTSAR	pBAD33-IpaC S17C	This study	This study
<i>S. flexneri</i> 2457T Δ ipaC	pTSAR	pBAD33-IpaC A38C	This study	This study
<i>S. flexneri</i> 2457T Δ ipaC	pTSAR	pBAD33-IpaC S63C	This study	This study
<i>S. flexneri</i> 2457T Δ ipaC	pTSAR	pBAD33-IpaC S101C	This study	This study
<i>S. flexneri</i> 2457T Δ ipaC	pTSAR	pBAD33-IpaC S103C	This study	This study
<i>S. flexneri</i> 2457T Δ ipaC	pTSAR	pBAD33-IpaC A106C	This study	This study
<i>S. flexneri</i> 2457T Δ ipaC	pTSAR	pBAD33-IpaC S108C	This study	This study
<i>S. flexneri</i> 2457T Δ ipaC	pTSAR	pBAD33-IpaC A119C	This study	This study
<i>S. flexneri</i> 2457T Δ ipaC	pTSAR	pBAD33-IpaC F136C	This study	This study
<i>S. flexneri</i> 2457T Δ ipaC	pTSAR	pBAD33-IpaC S156C	This study	This study
<i>S. flexneri</i> 2457T Δ ipaC	pTSAR	pBAD33-IpaC A161C	This study	This study
<i>S. flexneri</i> 2457T Δ ipaC	pTSAR	pBAD33-IpaC S177C	This study	This study
<i>S. flexneri</i> 2457T Δ ipaC	pTSAR	pBAD33-IpaC S271C	This study	This study
<i>S. flexneri</i> 2457T Δ ipaC	pTSAR	pBAD33-IpaC S286C	This study	This study
<i>S. flexneri</i> 2457T Δ ipaC	pTSAR	pBAD33-IpaC A313C	This study	This study
<i>S. flexneri</i> 2457T Δ ipaC	pTSAR	pBAD33-IpaC A328C	This study	This study
<i>S. flexneri</i> 2457T Δ ipaC	pTSAR	pBAD33-IpaC S349C	This study	This study
<i>S. flexneri</i> 2457T Δ ipaC	pTSAR	pBAD33-IpaC K350C	This study	This study
<i>S. flexneri</i> 2457T Δ ipaC	pTSAR	pBAD33-IpaC A353C	This study	This study
<i>S. flexneri</i> 2457T Δ ipaC	pTSAR	pBAD33-IpaC A354C	This study	This study
<i>S. flexneri</i> 2457T Δ ipaC	pTSAR	pBAD33-IpaC A358C	This study	This study
<i>S. flexneri</i> 2457T Δ ipaC	pTSAR	pBAD33-IpaC A363C	This study	This study
<i>E. coli</i> DH10B			Thermo Fisher ^a	
<i>S. Typhimurium</i> SL1344			Gift of C. Lee	
<i>S. Typhimurium</i> SL1344 Δ sipC			Gift of C. Lee	
<i>S. Typhimurium</i> SL1344 Δ sipC	pBAD18-SipC		This study	This study
<i>S. Typhimurium</i> SL1344 Δ sipC	pBAD18-SipC S18C		This study	This study
<i>S. Typhimurium</i> SL1344 Δ sipC	pBAD18-SipC A38C		This study	This study
<i>S. Typhimurium</i> SL1344 Δ sipC	pBAD18-SipC A126C		This study	This study
<i>S. Typhimurium</i> SL1344 Δ sipC	pBAD18-SipC S390C		This study	This study
<i>S. Typhimurium</i> SL1344 Δ sipC	pBAD18-SipC S394C		This study	This study
<i>S. Typhimurium</i> SL1344 Δ sipC	pBAD18-SipC S397C		This study	This study
<i>S. Typhimurium</i> SL1344 Δ sipC	pBAD18-SlpC A398C		This study	This study
<i>S. Typhimurium</i> SL1344 Δ sipC	pBAD18-SlpC A403C		This study	This study

^aCatalog no. 18290015.

bacteria. Lysates containing the bacteria were plated on agar plates with the appropriate antibiotics to quantify the number of intracellular bacteria.

Labeling of cysteines with PEG5000-maleimide. Individual IpaC or SipC amino acids were replaced with cysteines; native IpaC and native SipC both lack cysteines. For the analysis of the efficiency of

PEG5000-maleimide labeling of soluble IpaC, 2.5 mM PEG5000-maleimide was added to supernatants collected following induction of T3SS secretion with Congo red. The supernatant was incubated with PEG5000-maleimide at 30°C for 30 min. Samples were analyzed by SDS-PAGE and Western blotting; the efficiency of labeling was monitored by assessing the gel shift of IpaC.

For the analysis of cysteine labeling during infection, HeLa cells were seeded at 4×10^5 cells per well in a six-well plate. For each strain tested, 8×10^5 HeLa cells or 2.4×10^6 MEFs were used per experimental condition. Cells were washed once with 50 mM Tris (pH 7.4) supplemented with 150 mM NaCl and 1.2% arabinose. To enhance the efficiency of translocon pore insertion into the HeLa cell membrane, bacteria expressed the *E. coli* adhesion Afa-1 (7, 29). HeLa cells were infected with *S. flexneri* Δ ipaC bacteria producing individual IpaC cysteine substitution derivatives and Afa-1 or with *S. Typhimurium* Δ sipC bacteria producing individual SipC cysteine substitution derivatives at a multiplicity of infection of 200 in 50 mM Tris (pH 7.4) supplemented with 150 mM NaCl, 1.2% arabinose, and 2.5 mM PEG5000-maleimide. The bacteria were centrifuged onto the cells at $800 \times g$ for 10 min at 25°C and incubated at 37°C in humidified air with 5% CO₂ for 20 min. Cells were then harvested, and plasma membrane-enriched fractions were isolated, as done previously (7, 30). Briefly, the cells were washed three times with ice-cold 50 mM Tris (pH 7.4) and scraped in 50 mM Tris (pH 7.4) containing protease inhibitors (protease inhibitor cocktail, complete mini-EDTA free; Roche). Scraped cells were pelleted at $3,000 \times g$ for 3 min at 25°C. The pelleted cells were resuspended in 50 mM Tris (pH 7.4) containing protease inhibitors and 0.2% saponin and were incubated on ice for 20 min. For experiments testing the accessibility of IpaC residues in the presence of membrane permeabilization, PEG5000-maleimide was added in the presence of 0.2% saponin and not included during the infection. The suspension was centrifuged at $21,000 \times g$ for 30 min at 4°C. The supernatant, which contains the cytosol fraction, was decanted into a fresh tube. The pellet was resuspended in 50 mM Tris (pH 7.4) containing protease inhibitors and 0.5% Triton X-100, incubated on ice for 30 min, and centrifuged at $21,000 \times g$ for 15 min at 4°C. The supernatant from this spin contained the membrane fraction, and the pellet consisted of the detergent-insoluble fraction, which included intact bacteria. The efficiency of PEG5000-maleimide labeling was monitored by assessing the gel shift of IpaC or SipC by Western blotting. The following antibodies were used for Western blots: rabbit anti-IpaC (gift from Wendy Picking; diluted 1:10,000), rabbit anti-GroEL (catalog no. G6352; Sigma) (1:1,000,000), rabbit anti-caveolin-1 (catalog no. C4490; Sigma) (1:1,000), chicken anti-vimentin (catalog no. 919101; BioLegend) (1:5,000), mouse anti-SipC (gift from Jorge Galán; 1:10,000), goat anti-rabbit conjugated with horseradish peroxidase (HRP) (Jackson ImmunoResearch, catalog no. 115-035-003, 1:5,000), goat anti-mouse conjugated with HRP (catalog no. 111-035-003; Jackson ImmunoResearch) (1:5,000), donkey anti-chicken conjugated with HRP (catalog no. 703-035-155; Jackson ImmunoResearch) (1:5,000).

Statistical analysis. Except where specifically noted, all data are from three independent experiments, and the means \pm standard errors of the means (SEM) are presented. Dots presented within graphs represent independent experimental replicates. The means between groups were compared by a one-way analysis of variance (ANOVA) using GraphPad Prism 8 (GraphPad Software, Inc.). Alignment of IpaC and SipC was performed using Clustal Omega (20–22). Signal from Western blots was captured by film, film was digitized using an Epson Perfection 4990 photo scanner, and the density of bands was determined using ImageJ (National Institutes of Health).

SUPPLEMENTAL MATERIAL

Supplemental material for this article may be found at <https://doi.org/10.1128/mBio.00877-19>.

FIG S1, TIF file, 3.7 MB.

FIG S2, TIF file, 0.5 MB.

FIG S3, TIF file, 0.2 MB.

FIG S4, TIF file, 0.3 MB.

FIG S5, TIF file, 1.2 MB.

ACKNOWLEDGMENTS

We thank Jorge Galán, Wendy Picking, Denise Monack, and Cathy Lee for reagents and helpful discussions, Austin Hachey for technical assistance, and Daniel Kahne, D. Borden Lacy, Benjamin Spiller, Cammie Lesser, Amy Barczak, and the members of their laboratories for helpful discussions.

This work was funded by NIH grant AI081724 to M.B.G. and by NIH grants AI007061 and AI114162, the Massachusetts General Hospital Executive Committee on Research Tosteson Award, and the Charles A. King Trust Postdoctoral Research Fellowship Program, Bank of America, N.A., Co-Trustees, to B.C.R.

We declare that we have no conflicts of interest with the contents of this article.

The content is solely the responsibility of the authors and does not necessarily represent the official views of the National Institutes of Health.

REFERENCES

- Hu Y, Huang H, Cheng X, Shu X, White AP, Stavrinides J, Koster W, Zhu G, Zhao Z, Wang Y. 2017. A global survey of bacterial type III secretion systems and their effectors. *Environ Microbiol* 19:3879–3895. <https://doi.org/10.1111/1462-2920.13755>.
- Kubori T, Matsushima Y, Nakamura D, Uralil J, Lara-Tejero M, Sukhan A, Galan JE, Aizawa SI. 1998. Supramolecular structure of the *Salmonella typhimurium* type III protein secretion system. *Science* 280:602–605. <https://doi.org/10.1126/science.280.5363.602>.
- Blocker A, Gounon P, Larquet E, Niebuhr K, Cabiaux V, Parsot C, Sansonetti P. 1999. The tripartite type III secretin of *Shigella flexneri* inserts IpaB and IpaC into host membranes. *J Cell Biol* 147:683–693. <https://doi.org/10.1083/jcb.147.3.683>.
- Cheung M, Shen DK, Makino F, Kato T, Roehrich AD, Martinez-Argudo I, Walker ML, Murillo I, Liu X, Pain M, Brown J, Frazer G, Mantell J, Mina P, Todd T, Sessions RB, Namba K, Blocker AJ. 2015. Three-dimensional electron microscopy reconstruction and cysteine-mediated crosslinking provide a model of the type III secretion system needle tip complex. *Mol Microbiol* 95:31–50. <https://doi.org/10.1111/mmi.12843>.
- Epler CR, Dickenson NE, Bullitt E, Picking WL. 2012. Ultrastructural analysis of IpaD at the tip of the nascent MxiH type III secretion apparatus of *Shigella flexneri*. *J Mol Biol* 420:29–39. <https://doi.org/10.1016/j.jmb.2012.03.025>.
- Veenendaal AK, Hodgkinson JL, Schwarzer L, Stabat D, Zenk SF, Blocker AJ. 2007. The type III secretion system needle tip complex mediates host cell sensing and translocon insertion. *Mol Microbiol* 63:1719–1730. <https://doi.org/10.1111/j.1365-2958.2007.05620.x>.
- Russo BC, Stamm LM, Raaben M, Kim CM, Kahoud E, Robinson LR, Bose S, Queiroz AL, Herrera BB, Baxt LA, Mor-Vaknin N, Fu Y, Molina G, Markovitz DM, Whelan SP, Goldberg MB. 2016. Intermediate filaments enable pathogen docking to trigger type 3 effector translocation. *Nat Microbiol* 1:16025. <https://doi.org/10.1038/nmicrobiol.2016.25>.
- Lara-Tejero M, Galan JE. 2009. *Salmonella enterica* serovar Typhimurium pathogenicity island 1-encoded type III secretion system translocases mediate intimate attachment to nonphagocytic cells. *Infect Immun* 77:2635–2642. <https://doi.org/10.1128/IAI.00077-09>.
- Harrington A, Darboe N, Kenjale R, Picking WL, Middaugh CR, Birket S, Picking WD. 2006. Characterization of the interaction of single tryptophan containing mutants of IpaC from *Shigella flexneri* with phospholipid membranes. *Biochemistry* 45:626–636. <https://doi.org/10.1021/bi0512593>.
- Kuwae A, Yoshida S, Tamano K, Mimuro H, Suzuki T, Sasakawa C. 2001. *Shigella* invasion of macrophage requires the insertion of IpaC into the host plasma membrane. Functional analysis of IpaC. *J Biol Chem* 276:32230–32239. <https://doi.org/10.1074/jbc.M103831200>.
- Terry CM, Picking WL, Birket SE, Flentje K, Hoffman BM, Barker JR, Picking WD. 2008. The C-terminus of IpaC is required for effector activities related to *Shigella* invasion of host cells. *Microb Pathog* 45:282–289. <https://doi.org/10.1016/j.micpath.2008.06.003>.
- Wang F, Chan C, Weir NR, Denic V. 2014. The Get1/2 transmembrane complex is an endoplasmic-reticulum membrane protein insertase. *Nature* 512:441–444. <https://doi.org/10.1038/nature13471>.
- Radics J, Konigsmaier L, Marlovits TC. 2014. Structure of a pathogenic type 3 secretion system in action. *Nat Struct Mol Biol* 21:82–87. <https://doi.org/10.1038/nsmb.2722>.
- Bahrani FK, Sansonetti PJ, Parsot C. 1997. Secretion of Ipa proteins by *Shigella flexneri*: inducer molecules and kinetics of activation. *Infect Immun* 65:4005–4010.
- Armentrout EI, Rietsch A. 2016. The type III secretion translocation pore senses host cell contact. *PLoS Pathog* 12:e1005530. <https://doi.org/10.1371/journal.ppat.1005530>.
- Campbell-Valois FX, Schnupf P, Nigro G, Sachse M, Sansonetti PJ, Parsot C. 2014. A fluorescent reporter reveals on/off regulation of the *Shigella* type III secretion apparatus during entry and cell-to-cell spread. *Cell Host Microbe* 15:177–189. <https://doi.org/10.1016/j.chom.2014.01.005>.
- Lee JH, Park H, Park YH. 2014. Molecular mechanisms of host cytoskeletal rearrangements by *Shigella* invasins. *Int J Mol Sci* 15:18253–18266. <https://doi.org/10.3390/ijms151018253>.
- Garza-Mayers AC, Miller KA, Russo BC, Nagda DV, Goldberg MB. 2015. *Shigella flexneri* Regulation of ARF6 activation during bacterial entry via an IpgG-mediated positive feedback loop. *mBio* 6:e2584-14. <https://doi.org/10.1128/mBio.02584-14>.
- Bourdet-Sicard R, Rudiger M, Jockusch BM, Gounon P, Sansonetti PJ, Nhieu GT. 1999. Binding of the *Shigella* protein IpaA to vinculin induces F-actin depolymerization. *EMBO J* 18:5853–5862. <https://doi.org/10.1093/emboj/18.21.5853>.
- Sievers F, Higgins DG. 2014. Clustal omega. *Curr Protoc Bioinformatics* 48:3.13.11–3.13.16. <https://doi.org/10.1002/0471250953.bi0313s48>.
- Sievers F, Wilm A, Dineen D, Gibson TJ, Karplus K, Li W, Lopez R, McWilliam H, Remmert M, Soding J, Thompson JD, Higgins DG. 2014. Fast, scalable generation of high-quality protein multiple sequence alignments using Clustal Omega. *Mol Syst Biol* 7:539. <https://doi.org/10.1038/msb.2011.75>.
- Goujon M, McWilliam H, Li W, Valentin F, Squizzato S, Paern J, Lopez R. 2010. A new bioinformatics analysis tools framework at EMBL-EBI. *Nucleic Acids Res* 38:W695–W699. <https://doi.org/10.1093/nar/gkq313>.
- Du J, Reeves AZ, Klein JA, Twedt DJ, Knodler LA, Lesser CF. 2016. The type III secretion system apparatus determines the intracellular niche of bacterial pathogens. *Proc Natl Acad Sci U S A* 113:4794–4799. <https://doi.org/10.1073/pnas.1520699113>.
- Ide T, Laarmann S, Greune L, Schillers H, Oberleithner H, Schmidt MA. 2001. Characterization of translocation pores inserted into plasma membranes by type III-secreted Esp proteins of enteropathogenic *Escherichia coli*. *Cell Microbiol* 3:669–679. <https://doi.org/10.1046/j.1462-5822.2001.00146.x>.
- Klein JA, Dave BM, Raphenya AR, McArthur AG, Knodler LA. 2017. Functional relatedness in the Inv/Mxi-Spa type III secretion system family. *Mol Microbiol* 103:973–991. <https://doi.org/10.1111/mmi.13602>.
- Labrecq EH, Schneider H, Magnani TJ, Formal SB. 1964. Epithelial cell penetration as an essential step in the pathogenesis of bacillary dysentery. *J Bacteriol* 88:1503–1518.
- Miller KA, Garza-Mayers AC, Leung Y, Goldberg MB. 2018. Identification of interactions among host and bacterial proteins and evaluation of their role early during *Shigella flexneri* infection. *Microbiology* 164:540–550. <https://doi.org/10.1099/mic.0.000637>.
- Lu R, Herrera BB, Eshleman HD, Fu Y, Bloom A, Li Z, Sacks DB, Goldberg MB. 2015. *Shigella* effector OspB activates mTORC1 in a manner that depends on IQGAP1 and promotes cell proliferation. *PLoS Pathog* 11:e1005200. <https://doi.org/10.1371/journal.ppat.1005200>.
- Labigne-Roussel AF, Lark D, Schoolnik G, Falkow S. 1984. Cloning and expression of an afimbrial adhesin (AFA-I) responsible for P blood group-independent, mannose-resistant hemagglutination from a pyelonephritic *Escherichia coli* strain. *Infect Immun* 46:251–259.
- Scherer CA, Cooper E, Miller SI. 2000. The *Salmonella* type III secretion translocon protein SspC is inserted into the epithelial cell plasma membrane upon infection. *Mol Microbiol* 37:1133–1145. <https://doi.org/10.1046/j.1365-2958.2000.02066.x>.